

AN INSTRUMENT FOR NANOINDENTATION WITHOUT FRAME STIFFNESS DEPENDENCY

Jonathan D. Ellis, Stuart T. Smith, and Robert J. Hocken
Center for Precision Metrology
University of North Carolina at Charlotte
Charlotte, NC, USA

INTRODUCTION

Hardness is typically measured by indenting a specimen and then correlating the applied force to the projected area, surface area or depth of the indent. Because the hardness measurement requires force, displacement and sometimes geometric measurements, there are still many areas of discrepancy such as instrument frame deflection compensation, quantifiable units, traceable uncertainty, and geometrical errors in the indenter stylus. The purpose of this research is to establish a unique methodology for measuring hardness, nanohardness in particular, and address the aforementioned issues.

The measurement of nanohardness is of increasing value for several fields including thin-films for tool coatings and adhesives, micro-electrical mechanical systems (MEMS), and semiconductor process characterization. The goal of nanohardness measurements is to quantify material properties at the nanoscale. Some of the current techniques for calibrating nanohardness instruments require using material properties that are “known” on the macroscale. This is ambiguous because the material properties differ as the size-scale varies [1]. Additionally, the compliance variations within the instrument may vary considerably with scale and contribute to the uncertainty of the measurement.

A considerable contribution to the uncertainty of nanohardness measurement is the correlation between the indenter geometry and the depth of indent [2] and the characterization of the frame stiffness under loading. An alternative instrument design that reduces the dependency on frame stiffness will reduce the uncertainties in the force and depth measurements. In a typical instrument, the metrology loop and the force loop are largely coincident, Fig. 1. This coincidence is the source of the uncertainty associated with frame stiffness and thus, force and depth uncertainties. When the size of the indent is small, the stiffness of the indent may be

the same order of the magnitude as the stiffness of the frame and stage. In general, the deflections in the sample, frame, and stage behave similar to three springs in series, all nominally the same value because the stiffness of each element is comparable. By reducing the size of the metrology loop and removing a majority of the coincidence with the force loop, uncertainties can be estimated more accurately and at a lower magnitude.

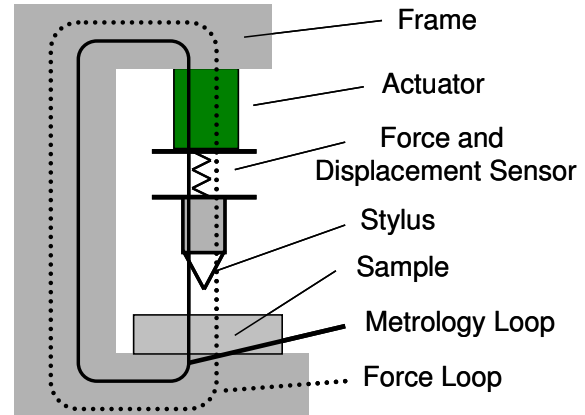


FIGURE 1: Coincident metrology and force loops within a C-Frame hardness measuring instrument.

Figure 2 depicts a new hardness instrument which significantly reduces the dependency on the frame stiffness. Because the area of the indent is difficult to measure directly at nanometer scales, as with other commercially available instruments, this instrument also measures the depth of indent as a function of applied force. Force is measured using a conventional load cell based on the displacement of a linear flexure of known stiffness. Measurement of the indenter penetration into the surface is obtained from a surface probe that is maintained at constant force. This force is maintained using a piezoelectric actuator (2nd actuator in Figure 2) as a load is applied to the indenter through the load cell. The depth of penetration is obtained from a displacement sensor that measures the translation of the second actuator. In this design,

deflections in the frame and stage are compensated and thus, a large contributor to uncertainty is significantly reduced.

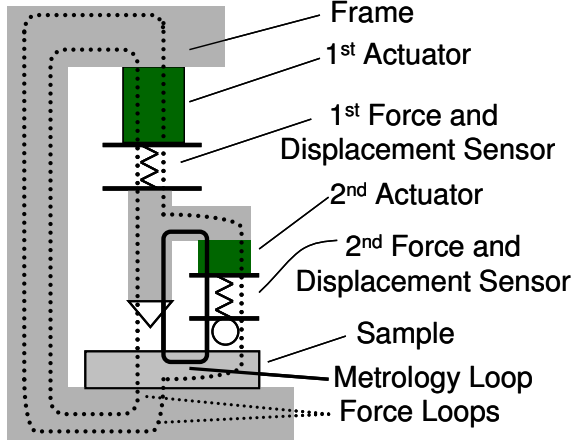


FIGURE 2: Hardness instrument compensating for frame and stage deflections where the metrology loop is much smaller than the force loops.

INSTRUMENT DESIGN

To measure nanohardness, this instrument requires a constant force feedback loop. This feedback is accomplished through an atomic force microscope (AFM) probe, shown as the second force and displacement sensor in Figure 2. The desired force level (pre-determined) is held constant using a piezoelectric transducer (PZT). Because the AFM probe does not deflect during an indent, calibration, although desired, is not necessary. The reference force mechanism is connected directly to the body of the indenter, shown in Fig. 3, and the load cell, F_{LC} , measures the total force from the indent, F_I , and the reference force, F_R .

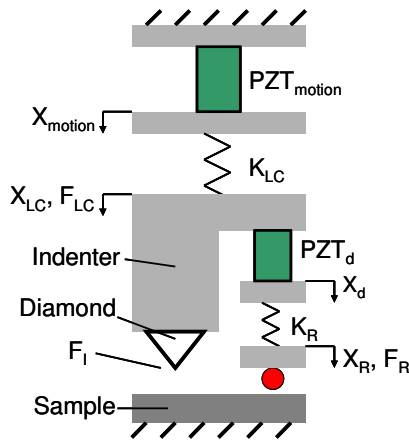


FIGURE 3: Theoretical model of an indentation instrument with a constant reference force mechanism to compensate for deflections in the instrument frame.

The force due to indentation is measured as the change in force and therefore does not include the reference force. Figure 4(a) illustrates the operation of the indenter during a simple indent showing the typical signal from the load cell during an indent cycle. The dashed line is the force due to the reference force, F_R , and the solid line is the force of the indent, F_I , and is used for determining the characteristics of the indent and subsequently the material properties.

When the indent occurs, the indenter stylus penetrates the surface of the sample and causes components in the force loop to deflect. Components in the metrology loop that coincide with the force loop deflect, causing errors in determining the displacement due to penetration versus displacement due to deflections. The displacement X_d is the total depth of indent plus the deflections of metrology loop. Because of the relatively high stiffness of the indenter body, deflections within the metrology loop are estimated to be insignificant compared with the depth of indent. Based on the idealized model of Fig. 3, the total depth of indent, X_h , is defined as

$$X_h = X_d - X_{met} \quad (1)$$

where X_d is the measured displacement of the servo (2nd actuator) and X_{met} is the deflection of metrology loop. The deflection of the metrology loop may be determined experimentally or estimated using analytic models but is considered insignificant in this case. The total depth of indent plus all deflections in the instrument, X_D , is

$$X_D = X_{motion} - X_{LC} \quad (2)$$

where X_{LC} is the deflection of the load cell and X_{motion} is the translation of the indenter and instrument frame. These measurements include an arbitrary vertical offset such that the measurement is zero when the indent begins, as noted in Fig. 4(b). By measuring these two signals simultaneously, as shown in Fig. 4(b), their difference shows the deflections in the frame and stage.

Once the depth and force of the indent is determined, the hardness is

$$H = \frac{F_I}{A(X_d)} = \frac{F_I}{aX_d^2} \quad (3)$$

where F_I is the force on the indent from Fig. 4(a), A is the area of indent, X_d is the depth of the indent extrapolated from Fig. 4(b), and a is a

correlation constant that depends on the indent stylus geometry and depth. Additional properties of the material can be found from the force-displacement curve, as shown in Fig. 5. From this curve, characteristics such as modulus [3], yield strength, and other mechanical properties can be determined [4]. This enables other phenomenon to be studied, such as adhesion across boundaries [5], phase transformations in silicon [6], or soft tissue samples [7].

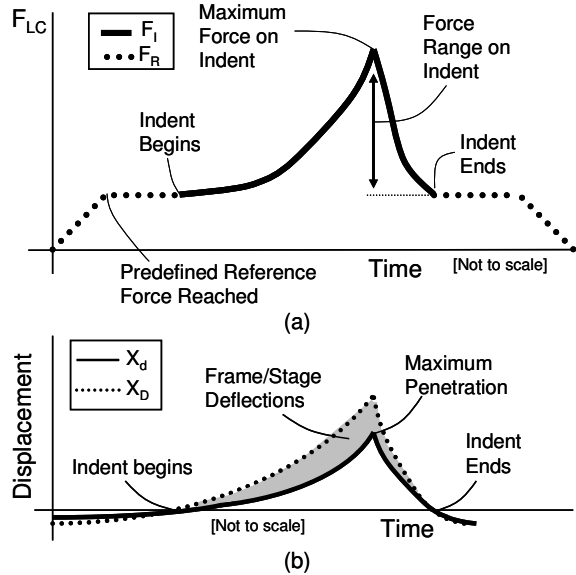


FIGURE 4: (a) Schematic of the force signal from the load cell during an indent sequence. The dashed line represents the force contributed by the reference sensor and the solid line is the force due to the indent. (b) Schematic of the measured depth of indent and the frame and stage deflections during indentation.

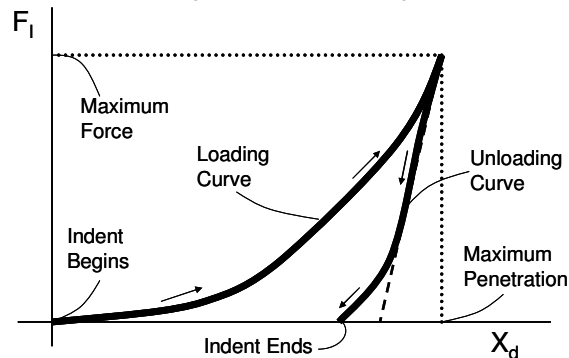


FIGURE 5: Loading and unloading curve compiled from the force extrapolated from Fig. 4(a) and from displacement (depth) from Fig. 4(b).

DESIGN SPECIFICATIONS

The purpose of this instrument is to have an accurate, traceable means of measuring hardness for nanometer scale indents. To achieve this, it is necessary to develop a

comprehensive estimate of combined uncertainty for any given measurement. In addition, a high natural frequency is desired to reduce susceptibility to vibration. A higher natural frequency also makes it possible to operate the instrument faster and with greater control. In this design, the natural frequency of the mass on the load cell spring, K_{LC} , is predicted to be greater than 85 Hz. Also, the load cell (a capacitance sensor) adds considerable damping with a predicted damping ratio of 0.35.

The three capacitance sensors (measuring X_{motion} , X_{LC} , and X_d) will be calibrated using a traceable Helium-Neon laser source which has an uncertainty of less than 1 part in 10^7 . To reduce errors in this calibration, the output of the capacitance sensor is fit to a polynomial therefore removing any periodic errors due to heterodyne beam mixing. Once the load cell sensor is calibrated, traceable weights will be used to determine its stiffness. Theoretically, the 0.07 nm (6σ) noise floor of the load cell combined with the stiffness of the load cell should result in a minimum force resolution of near 500 nN. The theoretical noise floor from X_d (depth of indent) is approximately 0.37 nm. Both of these displacement sensors will be bandwidth limited at 1000 Hz.

The reference force sensor is an AFM probe and the force and displacement values are not required, only that the values can be held at a constant value. Therefore, calibration of the ARM probe is not necessary. Given the resolution of the data acquisition system and a natural frequency approaching 2900 Hz for the PZT setup, a closed loop control on the position of the AFM should be able to compensate for less than nanometer deflections in the frame and stage at 500 Hz. A typical AFM probe has a stiffness less than 200 N m^{-1} and displacement resolutions better than 1 nm. Consequently, it is expected that the force can be held constant with deviations of less than $0.5 \mu\text{N}$.

Although nanohardness is intended for indents of less than 200 nm [8], the maximum depth of indent with this instrument will be approximately $7 \mu\text{m}$ and a maximum force of 50 mN.

While other instruments may state to resolve smaller displacement and force increments, the purpose of this instrument is to provide nanoscale hardness measurements with traceable uncertainties.

SIMPLIFIED UNCERTAINTY

Because the dependence on the frame and stage stiffness has been significantly reduced the uncertainty budget is simplified. The simplified expanded uncertainty in hardness, Equation (3), is

$$U_H^2 = \left(\frac{\partial H}{\partial F_i} \right)^2 \sigma_{F_i}^2 + \left(\frac{\partial H}{\partial X_d} \right)^2 \sigma_{X_d}^2 \quad (4)$$

The load cell and displacement sensor measurements are independent and therefore coupling terms are removed. The force and indent area coupled term can be found from finite element modeling. For materials of significantly lower modulus and hardness than diamond, this would typically be significantly less than the other uncertainty contributors and can therefore be considered zero.

The area function $A(X_d)$ is typically determined by using the geometry of an ideal Berkovich probe. In practice, there is no ideal probe due to manufacturing errors as well as an additional uncertainty contribution from the tip radii. Notwithstanding the problem of AFM tip deconvolution, it is possible that the indent area can be measured using a calibrated AFM [9]. Once the area is determined, effects of indenter orientation with respect to the central axis of the indenter can be evaluated mathematically. For an ideal Berkovich diamond a misalignment of 0.5 degrees, the change in area is 0.0022%. This increases nonlinearly with respect to the tip and tilt angles. For extreme misalignments of 5.0 degrees, the change in area only increases to 0.25%. These uncertainties will be measured and quantified prior to testing. However, determination of uncertainties in the correlation constants between depth and area represent a substantially unexplored challenge and require further research if these are to be verified in practice.

The uncertainties in the depth measurement include electrical noise in measuring X_d , thermal effects, Abbe offset between the indenter and the reference AFM, distortions of the components sharing the force and metrology loops (indenter body and indenter), and controller errors on the position of the AFM.

The majority of the uncertainty of the force measurement is from electrical noise in measuring X_{LC} , calibration of stiffness K_{LC} ,

thermal effects, and errors in the vibration isolation. Although the theoretical force resolution is 500 nN, the smallest reliable, traceable force measurement is only approximately 5 μ N [10], which represents the current limit for all instruments.

The detailed error budget has not been completed yet. Some of the uncertainties must await the construction and characterization of the instrument, which will be completed by the end of this year.

ROUND ROBIN TESTING

The instrument described here will be used for measurements at UNC Charlotte for the CIRP International Comparison of Nanoindentation. It consists of the measurement of three samples, single crystal aluminum, fused silica, and rolled tungsten, to determine the realization of the ISO Standards 14577-1, 2, 3.

REFERENCES

1. Pethica, J., Hutchings, R., and Oliver, W., 1983, Hardness measurements at penetration depths as small as 20 nm. *Philosophical Magazine*, 48: 593-606
2. Herrmann, K., Jennett, N., Wegener, W., Meneve, J., Hasche, K., and Seeman, R., 2000, Progress in determination of the area function of indenters used for nanoindentation, *Thin Solid Films*, 377-378: 394-400.
3. Doerner, M. and Nix, W., 1986, Interpreting data from depth sensing indentation instruments. *J. Mater. Res.*, 1: 601-609.
4. Bowden, F. and Tabor D., 1964, *The Friction and Lubrication of Solids: Part II*. Oxford University Press.
5. Daniels A., Smith S., and Lewis M., 1994, A scanning electron microscope based hardness indentation tester, *Rev. Sci. Instrum.*, 65: 632-638.
6. Kailer, A., Gogotsi, Y., and Nickel, K., 1996, Phase transformations of silicon caused by contact loading, *J. Appl. Phys.*, 81: 3057-3063.
7. Lim, C., Zhou, E., and Quek, S., 2006, Mechanical models for living cells – a review, *J. of Biomechanics*, 39: 195-216.
8. International Standard 14577-1, 2002
9. Herrmann, K., Jennett, N., Wegener, W., Meneve, J., Hasche, K., and Seeman, R., 2000, Progress in determination of the area function of indenters used for nanoindentation, *Thin Solid Films*, 377-378: 394-400.
10. Pratt, J., Kramar, J., Newell, D., and Smith, D., 2005, *Meas. Sci. Technol.*, 16:2129-2137.